ISSN 1560-0904, Polymer Science, Series B, 2023, Vol. 65, No. 4, pp. 487–495. © Pleiades Publishing, Ltd., 2023.
ISSN 1560-0904, Polymer Science, Series B, 2023. © Pleiades Publishing, Ltd., 2023.

FUNCTIONAL POLYMERS

Preparation and Characterization of New Soluble and Thermally Stable Polyazomethine by Polycondensation of Thiophene-2,5-dicarboxaldehyde and Ortho-tolidine for Optoelectronics

I. Bekri[a], H. Gherras[b], A. Dehbi[c,*], and A. Belfedal[a]

[a] *Laboratory of Physical Chemistry of Macromolecules and Biological Interfaces, Mustapha Stambouli University, BP 305, Mascara, 29000 Algeria*

[b] *Laboratoire de Chimie Organique, Macromoléculaire et des Matériaux (LCOMM), Faculté des Sciences Exactes, Université de Mascara, BP 763 Mascara, Algérie, 29000 Algeria*

[c] *Engineering Physics Laboratory, University Ibn Khaldoun, Bp 78, Zaaroura, Tiaret, 14000 Algeria*

**e-mail: abddehbi@gmail.com*

Received February 26, 2023; revised April 27, 2023; accepted June 2, 2023

Abstract—In recent years, there has been considerable interest in conducting polymeric materials containing conjugated bonds. Imine polymers, in which nitrogen atoms are incorporated into the conjugated system, offer a different approach to the formation of materials with equally interesting electronic and optical properties due to the –CH=N– group being isoelectronic with the –CH=CH– group. In this study, a polyazomethine copolymer was prepared by a polycondensation reaction using ortho-tolidine and thiophene-2,5-dicarboxaldehyde catalyzed by Maghnite H+. The effect of time, temperature, amount of Maghnite H+, and solvent on the produced copolymer material was investigated. The optical, structural, and morphological properties of the copolymer, as well as the size of the particles, were investigated using various techniques, including ^{1}H NMR and FTIR spectroscopy, thermogravimetric analysis, scanning electron microscopy, X-ray diffraction, and UV–Vis absorption. The optical band gap value was found to be around 2.54 eV.

DOI: 10.1134/S1560090423701038

INTRODUCTION

The field of organic electronics is concerned with the use of organic materials, rather than inorganic ones like silicon or gallium arsenide, to create electronic components and circuits. The discovery of the first conducting polymer in the late 1970s marked the beginning of this field, which was initially highly confidential. However, it now offers two major advantages over classical silicon-based electronics. Firstly, it allows the design of devices on flexible substrates, providing a wide range of new applications requiring substrate flexibility. Secondly, the costs of organic electronics are lower than those of the silicon route. Polymers with highly conjugated chains have been of particular interest to the scientific community, as they are materials of academic interest and promising candidates for a variety of applications. Numerous reviews have been published on conjugated systems such as polyacetylene, polyphenylenes, polyphenylenevinylenes, polypyrrole, polythiophene, and polyaniline [1].

Over the past few decades, scientists worldwide have devoted considerable efforts to synthesizing thermally stable polymers. Polyazomethines, also known as polyimines or Schiff base polymers, result from the polycondensation of diamine or hydrazine with dialdehyde or diketone. This class of polymers has nitrogen atoms with π conjugation spacers. These functional structures find application in various fields, including environmentally resistant materials due to their high stability, thermal properties, semi-conductivity, and antimicrobial and corrosion resistance applications. Although a few studies have been conducted on azomethine polymers and oligomers, Kaya and his research team have extensively investigated polymers such as poly(azomethine)s, poly(azomethine-urethane)s, poly(azomethine ester)s, poly(azomethine ether)s, poly(phenoxy-imine)s, and oligo(azomethine-ether)s [2]. In recent years, there has been significant research into the development of imine compounds. Some notable examples include a polycondensation reaction of naphthalene-1,5-diamine with aromatic aldehydes [3], the synthesis of pyrrole-carbazole-pyrrole monomers in four steps, which were then polymerized onto an ITO/glass surface via potentiodynamic and electrochemical process

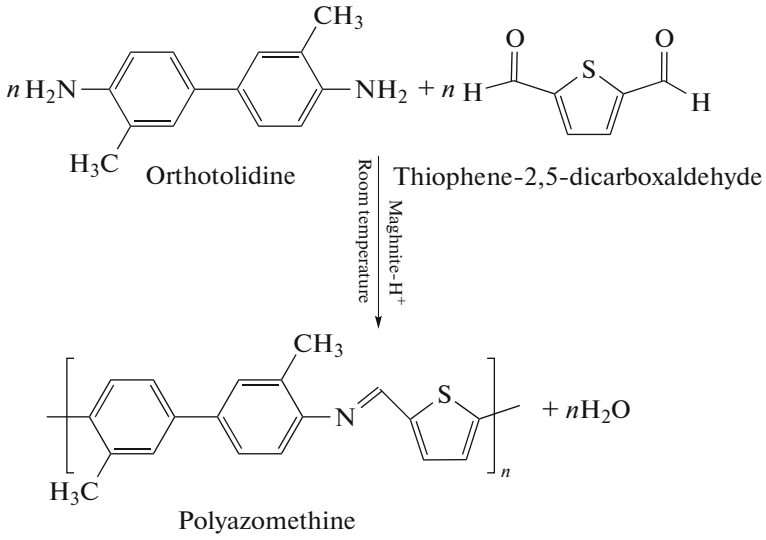

Scheme 1.

[4], a polycondensation reaction of poly(propylene imine) generation PPI with 2-pyrrole aldehyde [5], a polycondensation reaction of poly(phenoxy-Imine) with 3,5-diaminobenzoic acid, 4,4'-diaminobenzanilide, vanillin with 4-hydroxybenzaldehyde [6], the synthesis of 5-(4H-dithieno[3,2-b:2',3'-d]pyrrol-4-yl)naphthalen-1-amine by reacting 3,3'-dibromo-2,2'-bithiophene with 1,5-diamine naphthalene [7], and the condensation of 2,5-diamino-thiophene-3,4-dicarboxylic acid diethyl ester with five dialdehydes [8]. These studies have contributed significantly to the field of imine compounds and have opened up new possibilities for their use in various applications.

According to the literature, various catalysts have been used to synthesize different types of polyazomethines, including trifluoroacetic acid, trichloroacetic acid, difluoroacetic acid, formic acid, and acetic acid [9–11]. However, these catalysts are expensive, toxic, and difficult to neutralize. In this paper, we propose the use of a natural and efficient initiator that is non-toxic, has low environmental impact, and is easy to recover. This initiator is Maghnite-H+ (Mag-H+) in solution for polycondensation polymerization of Ortho-tolidine with Thiophene-2,5-dicarboxaldehyde.

The objective of this study is to synthesize a soluble conjugated polymer containing imine functionalities with a repeating unit (–N=CH–R'–CH=N–R–) that displays good electrical conductivity. The research also aims to investigate the impact of the –CH=N– group on the electronic properties and thermal stability of the newly developed polyazomethines. The synthesis of the polyazomethines will be carried out using a condensation reaction protocol that has been established by previous researchers [12].

EXPERIMENTAL

Ortho-tolidine (ORT) and thiophene-2,5-dicarboxaldehyde were purchased from Sigma-Aldrich Chemical Co. (Germany). The Mag-H+ catalyst was prepared in the laboratory by treating with a 0.5 M sulfuric acid solution. The chemicals used in the synthesis, including DMSO, acetone, DMF, sulfuric acid, chloroform, ethanol, toluene, and acetonitrile, were obtained from Merck Chemical Co. (Germany) and were used without further purification.

A 100 mL flask was used to prepare the reaction mixture by dissolving 1 mmol each of ortho-tolidine and thiophene-2,5-dicarboxaldehyde in 10 mL of chloroform, with 10 wt % of Mag-H+ added as a catalyst. The mixture was cooled in an ice bath for 30 min and then allowed to react for 24 h at room temperature under continuous stirring at 250 rpm. The reaction mixture was filtered to remove the Mag-H+ catalyst, and the resulting solution was slowly added dropwise to cold methanol to precipitate the copolymer. The copolymer was then vacuum dried at room temperature for 24 h. The % yield of the semiconductor copolymer obtained from the reaction was found to be 94.5%. The reaction scheme is shown in Scheme 1.

The number average molecular weight M_n and dispersity $Đ$ of synthesized copolymer were calculated using gel permeation chromatography; the obtained results are $M_n = 4830$ and $Đ = 1.33$.

The copolymer for this study was characterized using the following methods: solubility test results of the synthesized compounds are shown in Table 1, FTIR analysis, ^{1}H NMR analysis, X-ray diffraction, thermogravimetric analysis (TGA), scanning electron microscopy (SEM), and optical properties such as band gap (E_g) of PAZ were characterized by UV–Vis analysis and measurements. To optimize the parame-

ters and achieve a high reaction yield % of PAZ, several process parameters were studied. The key parameters included the choice of solvent, the molar ratio of the monomers, reaction time, temperature, ratio of catalyst to reagents, and the solubility test. By varying these parameters and evaluating their impact on the reaction yield, the optimal conditions for synthesizing high-quality PAZ were determined.

RESULTS AND DISCUSSION

FTIR spectroscopy was used to confirm the polycondensation reaction of the monomers and to identify the characteristic bands of the PAZ. Figure 1 shows the presence of two bands of ORT and one band of PAZ at 3470, 3374, and 3387 cm^{-1}, respectively, which are attributed to N–H stretching vibrations [13].

These vibrations are also observed at 825 and 807 cm^{-1}. The third band is observed at 3016 cm^{-1} for ORT and 3078 cm^{-1} for thiophene-2,5-dicarboxaldehyde, which corresponds to C–H stretching vibration of the aromatic units. The presence of a weak intensity band at 2787 cm^{-1} corresponds to the C–H band stretching symmetric of aromatic rings [14, 15] in the PAZ. The strong bands at 1650 cm^{-1} are assigned to the stretching of the imine function (C=N) of the PAZ [16–19], and they appear after the polymerization.

Table 1. Solubility test of synthesized copolymer (0.05 g in 10 mL)

Solvent	Test results
Chloroform	+
Dimethyl Formamide	+
Acetone	+
Toluene	+
Acetonitrile	+
Dimethyl Sulfoxide	+
Ethanol	–

Soluble (+), insoluble (–).

The characteristic bands of the aldehyde functional group in thiophene-2,5-dicarboxaldehyde and PAZ are observed at 1660 and 1733 cm^{-1}, respectively (C=O elongation vibrations) [15, 20]. The presence and stretching vibration of C=C and C–C bands are observed at 1520 and 1487 cm^{-1} of thiophene-2,5-dicarboxaldehyde and ORT, respectively. Similar results have been reported by [5, 21, 22]. The medium-

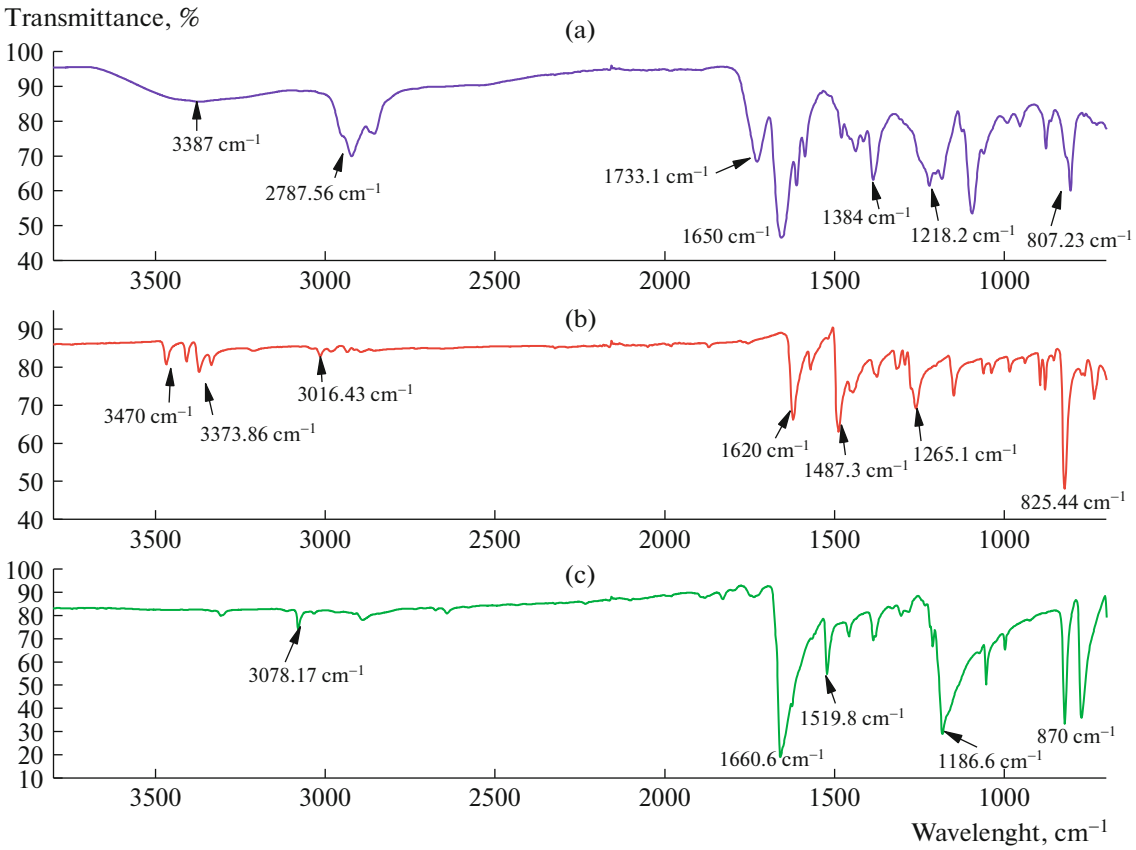

Fig. 1. FTIR spectrum of (a) PAZ, (b) ortho-tolidine, and (c) thiophene-2,5-dicarboxaldehyde.

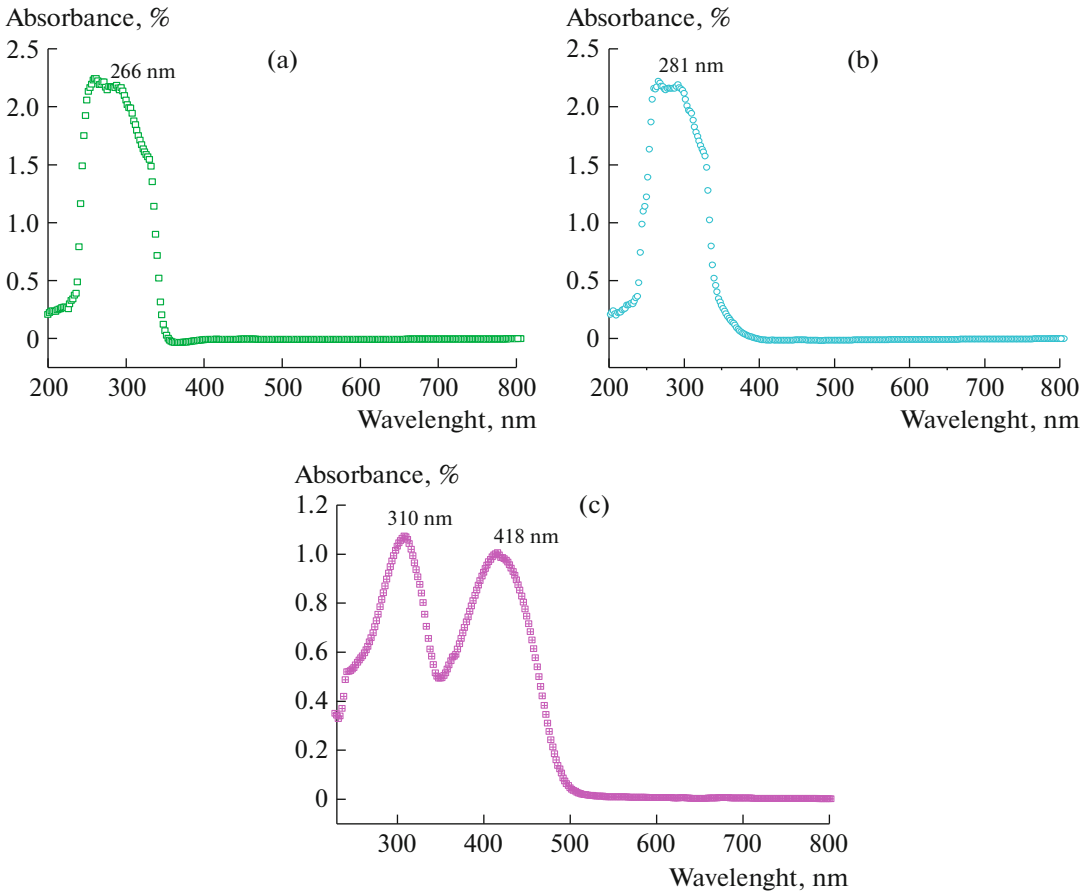

Fig. 2. UV–Visible absorption spectrum of (a) ortho-tolidine, (b) thiophene-2,5-dicarboxaldehyde, and (c) polyazomethine band.

intensity bands at 1265 and 1384 cm^{-1} are assigned to the stretching of C–N bands [19, 23, 24] in ORT and PAZ, respectively. The presence of C–S band of the thiazole ring in thiophene-2,5-dicarboxaldehyde and PAZ appears at 1187 and 1265 cm^{-1} [20, 25]. The appearance of N–H, C=O, C=N, and C–S bands confirms and indicates the success of the polycondensation reaction.

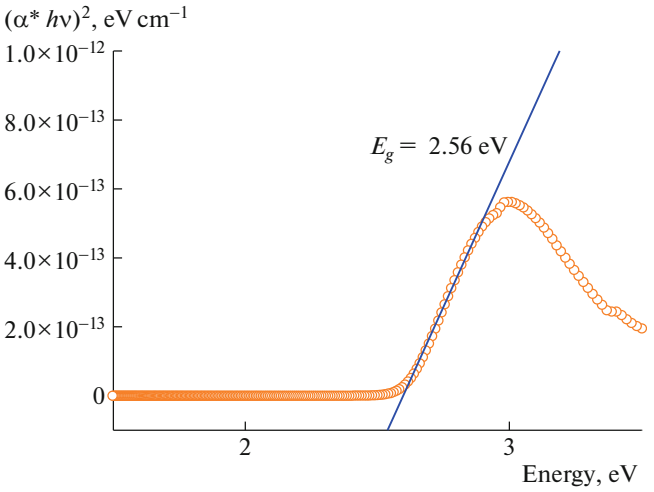

Fig. 3. The optical band gap variation separating the extreme of the valence and conduction.

The UV–Visible absorbance spectrum of PAZ dissolved in DMSO is presented in Fig. 2. The spectrum shows two strong absorption bands located between 250–350 nm (band 1) and 350–500 nm (band 2). Band 1 is attributed to the π–π* transitions of the thiazole ring [26], whereas band 2 is due to the *n*–π* transition of imine (–CH=N–) conjugations [2]. This denotes the optical gap energy of the copolymer, and indicates the synthesis of a completely new compound. Additionally, Fig. 3 displays the band gap of PAZ, which was extracted from the Tauc plot and found to be 2.54 eV. This result is consistent with previous research [27], indicating that our copolymer exhibits semiconducting properties. The UV–Vis spectrum of ORT and thiophene-2,5-dicarboxaldehyde shows two bands at 266 nm and 281 nm, respectively, probably due to the π–π* transitions of the benzene and thiazole units. Our results are consistent with the literature [28–30].

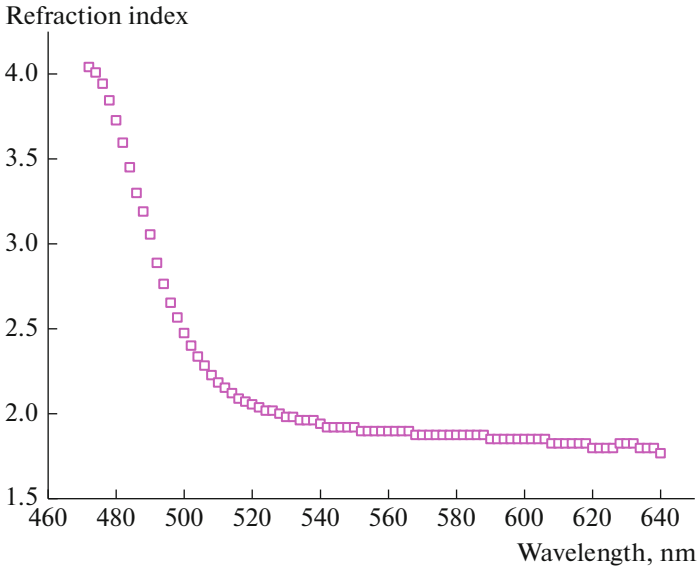

Fig. 4. Refractive index variation in UV-range of PAZ.

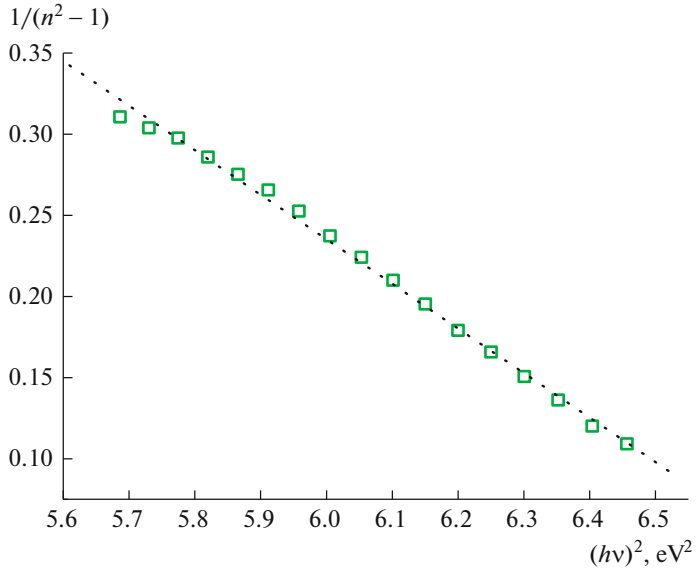

Fig. 5. Wemple and Didomenico model for determined the average gap E_M, dispersion energy E_D. $E_M = 2.62$ eV, $E_D = 1.45$ eV.

The dispersion parameters of the Sell-Meier plot, such as the single oscillator energy E_0 and dispersion energy E_D, were obtained by fitting the straight line in the $(n^2 - 1)^{-1}$ versus $(h\nu)^2$ plot, as shown in Fig. 4. Their values were calculated from the slope $(-1/E_0E_D)$ and intercept (E_M/E_D). The values of E_M and E_D were determined to be 2.62 and 1.45 eV, respectively. The Sellmeier equation calculates the wavelength-dependent refractive index based on a constant related to the absorption, using the Kramers-Kronig relationship between optical absorption and refractive index. The average oscillator wavelength λ_0 and the oscillator length strength S_0 were obtained by fitting the straight line in the $(n^2 - 1)^{-1}$ versus λ^{-2} plot, as shown in Figs. 5 and 6, respectively. Their values were calculated from the slope $(1/S_0)$ and the intercept $(1/\lambda_0^2 S_0)$. The values of λ_0 and S_0 were found to be 0.47 μm and 2.37 μm^{-2}, respectively.

The ^{1}H NMR spectra of the copolymer are presented in Fig. 7 and contain several types of signals assigned as follows: the singlet at 8.84 ppm is due to imine (–CH=N–) [31], while the multiple broad peaks between 7.31 and 8.09 ppm at positions a, b, and c are due to aromatic protons. The peaks between 6.66 and 6.69 ppm can be ascribed to protons on the positions d and e of the thiazole rings. The peak at

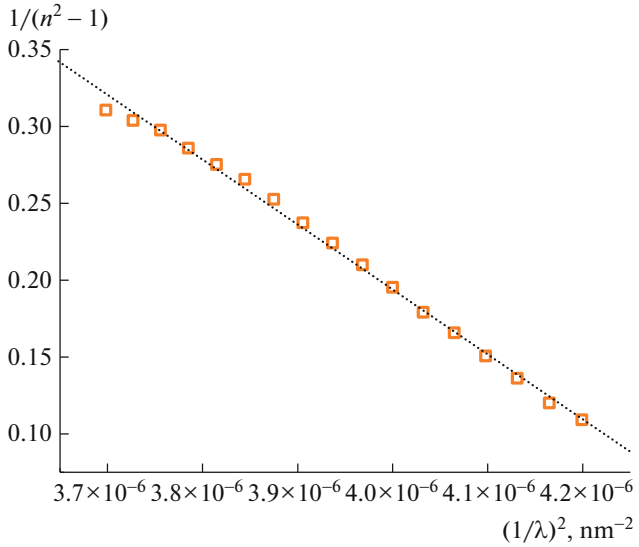

Fig. 6. Determination of the of average oscillator wavelength λ_0 and the oscillator length strength S_0 from $(n^2-1)^{-1}$ variation. $\lambda_0 = 0.47$ μm, $S_0 = 2.37$ μm^{-2}.

2.13 ppm is due to CH_3 proton. The peak present at 2.50 ppm represents the chemical shift of the solvent (DMSO-d6), and the water peak was at 5.00 ppm. Finally, we observed the presence of terminal aldehyde and amine functions at 10.00 and 3.36 ppm, respectively. The characteristic evidence, as provided by the UV–Visible spectra, IR spectra, and the ^{1}H NMR spectrum, confirmed the formation of the copolymer and supports the synthetic route adopted.

The thermal stability of conducting polymers is crucial for their potential applications. The sample was heated at a rate of 10 grad/min under a nitrogen atmosphere, and the thermogram (Fig. 8) shows a two-step weight loss. The first weight loss, which is between 0 and 5% up to 180–480°C, is likely due to the loss of moisture, residue, solvent, monomers, and low molecular weight [7, 16]. The second degradation occurs between 480–880°C, with a weight loss of 95%, and complete weight loss is observed at 1100°C [32]. The thermal analysis result indicates that PAZ has outstanding thermal stability.

Scanning Electron Microscopy (SEM) was used to examine the morphological properties of the synthesized PAZ. Figure 9 shows the SEM micrographs of PAZ. The particles exhibited irregular sizes and shapes with sharp edges distributed all over, indicating a heterogeneous surface. The particle size was small, located in the micro range, and these results were consistent with previous studies [33, 34], confirming the XRD results. The X-ray diffraction spectrum of the copolymer recorded in the powdered samples exhibited some additional small crystalline peaks in the spectrum at 2θ values of 12.93°, 14.68°, 15.64°, 17.95°, and 25.08° (Fig. 10), indicating the semi-crystalline nature of the copolymer synthesis [33].

Solubility tests were performed to ensure that the copolymer produced is soluble in the majority of organic solvents, as well as in other polyazomethines mentioned in the literature [35]. A quantity of solvent (in color) was added to a small amount of copolymer powder (orange color). All the results show the formation of a homogeneous orange solution, with the

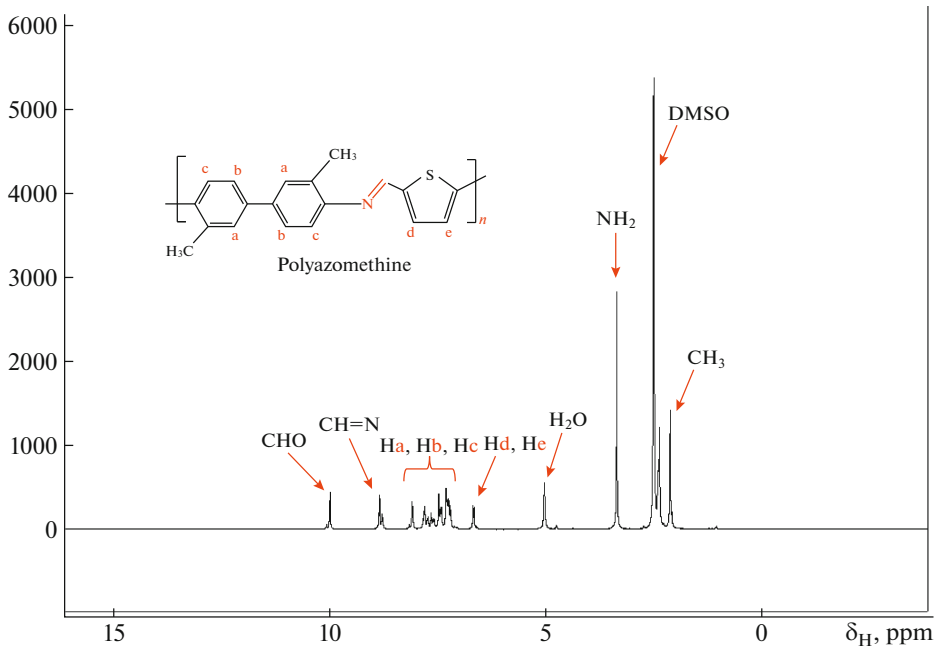

Fig. 7. ^{1}H NMR spectrum of PAZ.

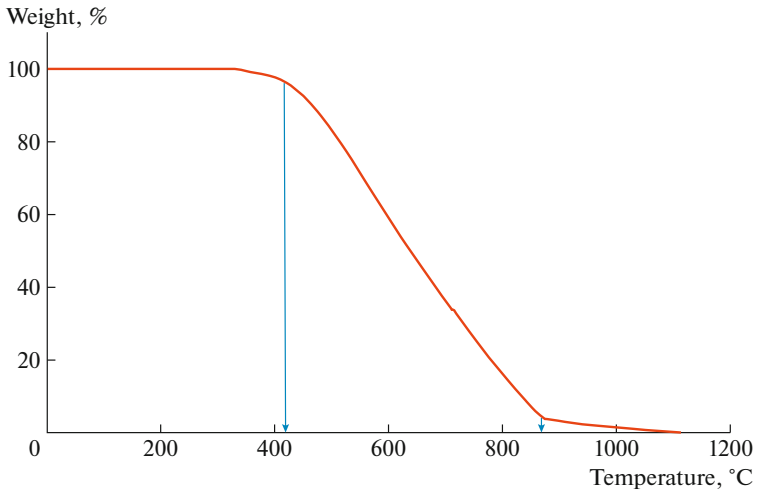

Fig. 8. Thermogravimetric analysis for PAZ.

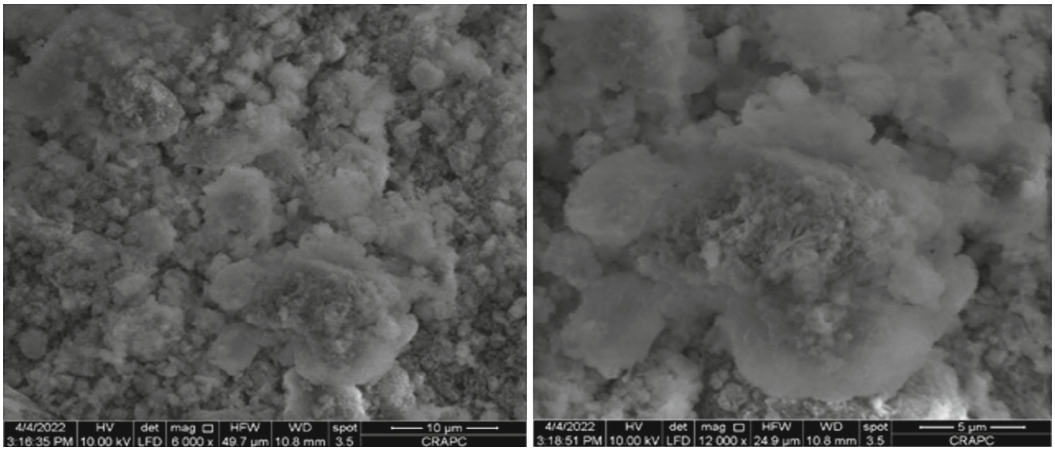

Fig. 9. The SEM images of PAZ.

exception of the ethanol solvent. These results clearly show that our polymer is soluble in most organic solvents such as indicate the test table, which again justifies the choice of this polymer for several technological applications. The yield of polymerization (by condensation) of PAZ in the presence of 10 wt % of Mag-H+ as a function of time is presented in Fig. 11. The graph shows two stages of polymerization. During the first phase (from 2 to 20 h), the yield percentage increases with time. The curve then shows a plateau during the second phase (from 20 to 28 h), indicating an excellent rate. Therefore, the optimum polymerization time was found to be 24 h, which gave a yield of 94.47% and was fixed for the remainder of this study.

A significant effect of the polymerization temperature on the copolymer yield is shown in Table 2. Four experiments were performed at different temperatures. As the temperature increased from 20 to 60°C, the

Table 2. The effects of different parameters on the reaction of PAZ

Parameters													
temperature, °C				molar/ratio (ORT/2-5 Thio)					Mag-H+ (% by weight)				
20	30	40	60	20/80	40/60	50/50	60/40	80/20	3	5	7	10	15
Yield, %													
67.9	51.3	32.0	29.6	35.6	49.6	57.2	42.8	29.3	64.0	77.4	84.0	93.2	88.5

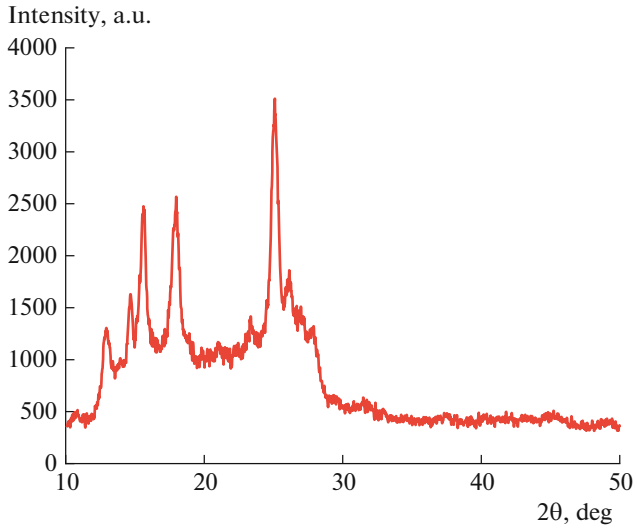

Fig. 10. XRD scans spectrum of PAZ.

yield decreased from 67.92% to about 29.58%. This behavior suggests that the optimum polymerization reaction temperature is around 20°C. Table 2 also shows the amount of Mag-H+ used, which includes various weight ratios of Mag-H+/monomer. The addition of more clay decreases the yield, and the maximum yield of 93.23% is reached for 10 wt% of Mag-H+. This tendency is likely the result of the number of initiator active sites to induce polymerization, which is proportional to the amount of catalyst used in the reaction [13].

The copolymer was synthesized using different molar ratios of ORT and thiophene-2,5-dicarboxaldehyde, as shown in Table 2. It is clear that the copolymer was greatly influenced by the monomer ratios, and it shows the highest yield at a 50/50 monomer ratio. When the amount of either of these two monomers increases, the polymerization rate decreases.

The solvent effect on PAZ polymerization was observed, and the reaction was carried out in acetone (dielectric constant = 20.7), dimethyl sulfoxide (DMSO) (dielectric constant = 46.67), and chloroform (dielectric constant = 4.81). The rate of polymerization in DMSO was found to be higher (95.12%) than in the other solvents, as shown in Table 3.

CONCLUSIONS

The synthesis and polymerization of a novel polyazomethine using ortho-tolidine and thiophene-2,5-dicarboxaldehyde monomers through condensation reaction with Mag-H+ as a catalyst have been successfully achieved. The synthesized copolymer exhibits similar morphological and optical properties, yet different electrical and thermal characteristics. The structure of the copolymer was confirmed by TGA, X-ray diffraction, FTIR, ^{1}H NMR, and UV–Vis analyses. The copolymer has a bandgap of approximately 2.54 eV, indicating its potential use in electrical, optoelectrical, electrochemical, and photovoltaic applications due to its semiconducting properties. The FTIR results confirm the occurrence of the polycondensation reaction with the appearance of the C=N band. Based on TGA and X-RD analysis, the copolymer shows a semi-crystalline structure and good thermal stability, which make it suitable for applications at higher temperatures. The yield% of the reaction can be improved by optimizing the parameters such as time

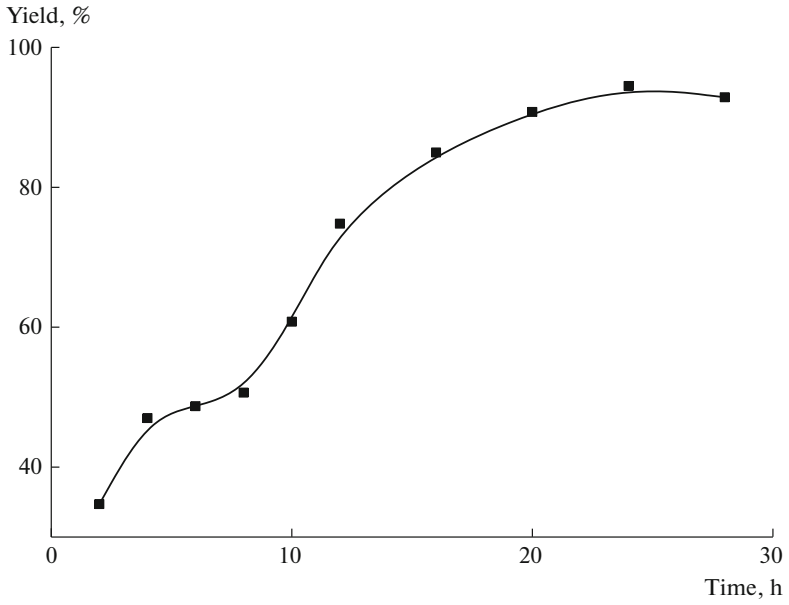

Fig. 11. The yield % of the PAZ copolymer versus time for polymerization reaction.

Table 3. Effect of the solvent on the polymerization

Solvent	Chloroform	Acetone	Dimethyl Sulfoxide
Dielectric constant	4.81	20.7	46.67
Yield, %	94.47	91.34	95.45

(24 h), temperature (20°C), catalyst (10 wt % of Mag-H+), DMSO as solvent, and 50/50 molar ratio of the monomers.

FUNDING

This work was financially supported by the Agency Thematic Research Science and Technology (ATRST), the Directorate General of Scientific Research and Technological Development (La Direction Générale de la Recherche Scientifique et du Développement Technologique (DGRSDT)) of Algeria.

CONSENT OF INTEREST

The authors declare that they have no conflict of interest.

REFERENCES

1. M. Grigoras and C. Catanescu, J. Macromol. Sci. C **44**, 37 (2004).
2. I. Kaya and F. Yener, Arab. J. Sci. Eng. **44**, 6339 (2019).
3. I. Kaya and M. Yıldırım, Polym. J. **50**, 5653 (2009).
4. O. Denizis, F. Koyuncu, K. Sermet, and O. Eyup, Polym. J. **51**, 1663 (2010).
5. A. Baleg, M. Nazeem, A. Omotayo, N. M. Stephen, R. H. Nicolette, G. Priscilla, and I. Emmanuel, J. Electroanalyt. Chem. **652**, 18 (2011).
6. S. Dilek and I. Kaya, Arab. J. Sci. Eng. **6**, 2381 (2017).
7. S. Dilek and I. Kaya, Mater. Chem. Phys. **237**, 121876 (2019).
8. A. Pajak, S. Kotowicz, P. Gnida, J. G. Małecki, A. Ciemięga, A. Łuczak, J. Jung, and E. Schab-Balcerzak, Int. J. Molec. Sci. **23**, 8160 (2022).
9. P. Prasit, T. Motohiro, and K. Takaomi, Sens. Actuators, B **209**, 186 (2015).
10. H. Yusuke and K. Takaomi, J. Eng. **4**, 139 (2012).
11. A. Sirilak, S. Kawee, and L. Sarintorn, J. Metal. Mater. Mineral. **24**, 29 (2014).
12. H. Gherras, A. Yahiaoui, A. Hachemaoui, A. Belfedal, A. Dehbi, and A. Mourad, J. Semicond. **39**, 1 (2018).
13. H. Gherras, A. Yahiaoui, A. Hachemaoui, A. Belfedal, A. Dehbi, and A. Zeinert, Polym. Polym. Compos. **28**, 265 (2019).
14. S. Benguella, A. Hachemaoui, A. Yahiaoui, and A. Dehbi, Polym. Sci., Ser. B **62**, 697 (2020).
15. L. Bai, X. Yan, F. Bingwei, Z. Junping, Composites, Part B **223**, 109 (2021).
16. M. Bıyıkoglu and H. Ciftc, Polym. Bull. **70**, 2843 (2013).
17. L. Fu-han, J. Bai, Y. Guang, M. Fang-hong, H. Yan-jun, and N. Hai-jun, Adv. Mater. **31**, 1 (2019).
18. F. Song, Z. Li, P. Jia, M. Zhang, C. Bo, G. Feng, L. Hua, and Y. Zhou, J. Mater. Chem. A **7**, 13400 (2019).
19. L. Mouacher, A. Yahiaoui, A. Hachemaoui, A. Dehbi, and A. Benkouider, Polym. Sci., Ser. B **63**(3), 314 (2021).
20. J. Nam, W. Jang, K. K. Rajeev, J.-H. Lee, Y. Kim, T.-H. Kim, J. Power Sources **499**, 229968. (2021).
21. M. Abbas, A. Hachemaoui, A. Yahiaoui, A. Mourad, A. Belfedal, N. Cherupurakal, Polym. Polym. Compos. **29**, 982 (2021).
22. B. Alouche, A. Yahiaoui, A. Dehbi, and A. Hachemaoui, Polym. Sci., Ser. A **63**, 865 (2021).
23. B. Alouche, A. Yahiaoui, and A. Dehbi, Polym. Sci., Ser. B **62**, 750 (2020).
24. V. Gayathri and R. Balan, J. Environm. Nanotech. **8**, 20 (2019).
25. X. Shen, H. Haiming, L. Hang, L. Ruiyang, H. Texiong, W. Dezhi, Z. Peng, and Z. Jinbao, Polymer **201**, 122568 (2020).
26. H. Ciftci, H. Testereci, and Z. Oktem, Polym. Bull. **66**, 747 (2011).
27. G. Zotti, A. Randi, S. Destri, W. Porzio, and G. Schiavon, Chem. Mater. **14**, 4550 (2002).
28. S. Koyuncu, I. Kaya, F. Koyuncu, and O. Eyup, Synt. Met. **159**, 1034 (2009).
29. A. Iwan, B. Boharewicz, I. Tazbir, M. Malinowski, M. Filapek, T. Kłąb, B. Luszczynska, I. Glowacki, K. P. Korona, M. Kaminska, J. Wojtkiewicz, M. Lewandowska, and A. Hreniak, Solar Energy **117**, 246 (2015).
30. I. Kaya, N. Cıtakoglu, and F. Kolcu, Polym. Bull. **74**, 1343 (2016).
31. S. Destri, M. Pasini, C. Pelizzi, W. Porzio, G. Predieri, and C. Vignali, Macromolecules **32**, 353 (1999).
32. L. Ravikumar, I. Pradeep, R. Thangaiyan, and M. Balachandran, Int. J. Polym. Mat. Polym. Biomat. **61**, 288 (2012).
33. A. Khan Asif and I. Khan Anish, Talanta, **72**, 699 (2007).
34. H. Zou, L. Wang, X. Wang, L. Pengfei, and L. Yaozu, Polymers **8**, 407 (2016).
35. A. Vlad, M. Cazacu, G. Munteanu, A. Anton, and B. Petru, Eur. Polym. J. **44**, 2668 (2008).